Doping effects on metallic and semiconductor single wall carbon nanotubes

Francesco Buonocore

Doping effects on metallic and semiconductor single wall carbon nanotubes

Journal:	*Philosophical Magazine & Philosophical Magazine Letters*
Manuscript ID:	TPHM-06-Aug-0279
Journal Selection:	Philosophical Magazine
Date Submitted by the Author:	04-Aug-2006
Complete List of Authors:	Buonocore, Francesco; STMicroelectronics
Keywords:	electronic structure, first-principles calculations, carbon nanotubes
Keywords (user supplied):	doping

Doping effects on metallic and semiconductor single wall carbon nanotubes

F Buonocore

STMicroelectronics, c/o IMAST, Piazzale Enrico Fermi 1, Porto del Granatello, 80055 Portici (NA), Italy

E-mail: francesco.buonocore@st.com

Keywords: electronic structures, first-principles calculations, carbon nanotubes, doping.

PACS: 71.15.Mb; 71.55.-i ; 73.22.-f; 81.05.Tp.

Abstract

In this paper we investigate nitrogen and boron doped zig-zag and armchair single wall carbon nanotubes (SWNTs) with theoretical models based on the density functional theory. We take into account nitrogen and boron doping for two isomers in which substitutive atoms are on opposite sides of the tube, but only in one isomer the impurity sites are symmetrical with respect to the diameter. The band structures show a strong hybridization with impurity orbitals that change the original band structure. Although the two isomers of armchair SWNT exhibit the same formation energy, their band structures are different. Indeed asymmetrical isomers are gapless and exhibit a crossing of valence and conduction bands at k=π/a, leading to metallic SWNTs. Band structures of symmetrical isomers, on the other hand, exhibit an energy gap of 0.4 eV between completely filled valence band and empty conduction band. We use density of charge in order to understand this difference. In zig-zag SWNT an impurity band is introduced in the energy gap and for N doping this band is just partially occupied in such a way that the electronic behaviour is reversed from semiconductor to metallic. While for a given isomer armchair SWNT shows similar behaviours of N and B doped structures, B doped zig-zag SWNTs present different band structure and occupation compared to the N doped case.

1. Introduction

Doping is currently used in the Ultra Large Scale Integration (ULSI) technology in order to form junctions that according to the request of the devices roadmaps are evolving towards ultrashallow junctions and nanojunctions. Because of the limit of the actual technology, different solutions have been proposed. Among them, the use of carbon nanotubes (CNTs) has been proved to reach figure of merit in the field effect devices that are even higher with respect to the silicon technology. However, the high contact resistance of the metal/nanotube interfaces limits the possibility to exploit the superior properties of the CNTs. Doping can be very useful to control the electrical properties of carbon nanotubes. Moreover several applications of doped CNTs have been suggested such as field emission sources [1]-[2], sensors [3] and composites.

Usually nitrogen (N) and boron (B) are introduced to dope CNTs. It has been found [4]-[5] that N doping (B doping) of single wall carbon nanotubes (SWNTs) at low concentrations introduces impurity levels below the conduction band (above the valence band) for semiconductor SWNTs and below (above) the first van Hove singularity above (below) the Fermi level for metallic SWNTs.

B or N doped CNTs can be synthesized with techniques similar to those used for producing pure CNTs, that are arc discharge [6]-[9], laser ablation [10] and chemical vapor deposition (CVD) [11-14]. It is likely that three coordinated (substitutive) B impurity are formed in the graphite structure of the CNT surface [1], while two binding types were demonstrated to be possible for N impurity: twofold coordinated (pyridine impurity) and threefold coordinated in an sp^2-like fashion (substitutive impurity) [14], [15]. STM measurements [16] showed that local density of states (LDOS) can be non-zero at the Fermi energy on the surface of N doped multi-wall carbon nanotubes (MWNTs) and this is a sign of a metallic behaviour, corresponding to a superior conductance.

In all of the techniques we have mentioned the control of doping density and morphology is far to be reached and still more work has to be done. For example the topological structure of N-doped CNTs growth by CVD is not crystalline and looks like hollow nanofibers with stacked-cone or compartmental morphology (so–called bamboo-like) [11]–[13]. However very recent dynamics simulations [17] have shown it is possible to produce crystalline doped nanotubes by low-energy ion irradiation. Substitutive N and B impurities are predicted at low energy. Simultaneously an experimental work was published by Yamamoto *et al* [18], where they showed development of a mass-separated low-energy ion beam irradiation system under ultra high vacuum, used to dope SWNTs. At low ion density the preserved crystallinity of SWNTs was clear and the three-coordination of the nitrogen was evidenced at high ion density, when the electron energy loss spectrum (EELS) of nitrogen can be distinguished. The cited works pave the way to controlling doping of crystalline SWNTs.

Doped SWNTs have been theoretically investigated in several papers. Lammert *et al* [4] investigated disordered substitution of boron and nitrogen at concentrations of 3.5% and 1.4%, and calculated both donor and acceptor levels in the gap. Nevidomskyy *et al* [5] have calculated the electronic structure of very large N doped SWNTs in such a way to study the isolated substitutive impurity. Kang *et al* [19] studied N impurities in several configurations in (5,5) and (10,0) SWNTs, where the concentration for substitutive impurity was 2.5%.

In the following sections we calculate from first principles the band structures of substitutive N and B doped zig-zag and armchair SWNTs with two impurities per unit cell in two configurations where impurities are on opposite sides of the tube but with different relative positions. Although in both configurations the interaction between the two impurities is weak, we will see that in armchair SWNT the resulting bands are not simply related to the concentration of the impurities, but also to the way in which N or B atoms are distributed in the unit cell. In order to understand modifications of the CNT properties due to doping we will observe how band structure and occupation change with respect to those of the pure nanotube.

It is evident that in order to have a realistic description of doped CNTs a random distribution of impurities should be used. However we suppose that an ideal situation in which impurities are distributed in a periodic cell can provide some useful insights on the doping effects in a less computationally expensive way.

2. The theoretical model

In this paper we investigate N and B substitutive doping of zig-zag and armchair SWNTs. We used a supercell of 80 atoms that is four times the natural unit cell of the pure armchair (5,5) SWNT and another one of 96 atoms that is three times the natural unit cell for pure zig-zag (8,0) SWNT. Considering that we are setting up two impurities per supercell, the mentioned SWNTs correspond to impurity concentrations of 2.5% and 2.1%, respectively. The supercell of the (5,5) ((8,0)) SWNT is tetragonal with edges a= 15.0 Å, b= 15.0 Å, c= 9.76 Å (c= 12.65 Å). The large distance between the CNT and its image in neighboring cells allows neglecting inter-tube interactions.

The substitutive impurity positions are shown in figure 1 for both the (5,5) and (8,0) SWNT. It is seen that two possible isomers, AZ and AA', are considered, in which the two impurities are placed at different or same height along the nanotube axis, respectively. (5,5) SWNT with AA' structure is also treated in reference [19].

Our theoretical investigation on doped SWNTs was carried out with calculations based on the density functional theory (DFT) within the generalized gradient approximation (GGA) with the Perdew, Burke and Ernzerhof (PBE) [20] correlation functional. Our calculations are closed shell and were done using the DMol^3 program [21]. The electronic wavefunctions are

expanded in atom-centered basis functions defined on a dense numerical grid. The chosen basis set was DND (Double Numerical plus d-functions) [22]. DND is an all-electron basis set composed of two numerical functions per valence orbital, supplemented with a polarization function. Each basis function was restricted to a cutoff radius. A global real space cutoff is selected as a maximum value of the cutoffs specific for every element of the system. Real space cutoffs for atomic species were optimized by considering total energies of atoms. The chosen cutoff values lead to atomic energies with an accuracy of 0.1 eV/atom, allowing calculations without a significant loss of accuracy. All geometry optimizations were performed using a scheme based on delocalized internal coordinates generalized to periodic boundary conditions [22], and Brillouin-zone integrations were performed using a 1 x 1 x 3 Monkhorst-Pack (MP) grid [23]. We have chosen a 3×3×20 MP k-point grid to calculate the density of states (DOS), and we used the linear interpolation method [24] to provide an improved representation of the DOS. An instrumental broadening of 50 meV has been introduced.

3. Results and discussion

3.1. N and B doped zig-zag (8,0) carbon nanotubes

The band structure of the pure (8,0) SWNT is shown in figure 2 panel b. It is well known that zig-zag (8,0) SWNT is semiconductor with an energy gap of 0.71 eV as calculated within GGA. After the optimization of the geometries we calculated the formation energy of the investigated systems defined as E(SWNT(X doped)) – E(SWNT(pure)) + 2E(C) - 2E(X) (X=N or B), where E is the total energy of the specified system. The formation energies of doped (8,0) SWNT are reported in table 1. Very similar results are obtained for the two isomers, for both N and B doping.

[Insert table 1 here]

The lengths of the N-C and B-C bonds of the optimized geometries are reported in table 2 and compared with those of the pure SWNT. A small variation of the structures is found for N doped SWNTs, while the lengths of B-C bonds have a 6% increase with respect to those of the pure SWNT. In fact B atom forms three σ bonds with the adjacent C atoms and do not have π bonding, differently from C atoms. Therefore B-C bond lengths are larger than those of N-C and C-C bonds. A structural deformation is found with a slight outward displacement of the B atom out of the tube. According to what obtained for the formation energy (see table 1), no significant difference is found between AZ and AA' isomers.

[Insert table 2 here]

Due to the overlap of the impurity orbitals in the periodic structure we expect an impurity band rather than a set of discrete levels as in weak doping. The band structures of the doped (8,0) SWNTs are shown in figure 2. All of the bands we plot are just in an energy window of 3.5 eV around Fermi energy. The results for AZ and AA' isomers are again very similar. The substitutive N doping shifts the Fermi energy upward in such a way to intersect the impurity band labeled as F that becomes conductive and the band below, making another band available to the conduction. The same results have been confirmed by calculations on (7,0) SWNT. We have verified from LDOS calculations that atomic orbitals of the N atoms contribute to the impurity band. On the other hand, for substitutive B doping the Fermi energy is shifted downward and an empty impurity band labeled as G appears above the completely filled valence band. For both AZ and AA' structures we have very small indirect energy gaps (a few meV), with the top (bottom) of the valence (conduction) band located at k=0 (k=π/c). The finite value at the Fermi energy of the DOS reported in figure 3 panel a indicates that the B doped SWNT is a metal.

3.2. N and B doped armchair (5,5) carbon nanotubes

Armchair (5,5) SWNT is metallic because valence and conduction bands cross at the Fermi energy and just infinitesimal excitations at finite temperatures suffice to excite carriers in the conduction band. These features are in agreement with the numerical tight binding rules according to which the (n_1,n_2) SWNT is metallic when $n_1-n_2=3j$ with j integer and semiconductor otherwise [25] and are confirmed by our DFT calculations shown in figure 4. The formation energy of N and B doped (5,5) SWNT are shown in table 3. Isomers of B doped (5,5) SWNT demand a formation energy smaller than those for (8,0) SWNT.

[Insert table 3 here]

The lengths of the N-C and B-C bonds of the optimized geometries are reported in table 4. Small modification of the structures for N doped SWNTs and 6% increase respect those of the pure SWNT for B doped SWNT are found as in the previous case, confirming the slight outward displacement of the B atom out of the tube.

[Insert table 4 here]

We have also calculated the band structure of the (5,5) SWNT with substitutive N and B doping, as shown in figure 4. The Fermi energy shifts to higher (lower) energy for N (B) doping and the band structure displays a quite complicated hybridization of the impurity orbitals with the pure SWNT π orbitals. We observe that in both structures the energy gap at k=0 undergoes a huge reduction from 1.8 eV to 0.4 eV compared to the pure SWNT. The band structures in AZ and AA' isomers are quite similar, except for the behavior at the right edge of the Brillouin zone. Indeed valence and conduction bands of the AZ isomer cross at $k=\pi/a$ rather than $k=2\pi/3a$ as in the pure SWNT, while for the AA' isomer we have an energy gap above Fermi energy for any k value. Therefore, doped SWNTs considered in this work display metallic or semiconductor behaviours according to the impurities position (AZ and AA' isomers, respectively). To confirm that AZ isomer is metallic we have calculated the DOS in figure 3 panel b that shows a finite value at the Fermi energy. The energy gap in AA' isomer was not pointed out in the same system by Kang et al. [19] for (5,5) SWNT.

In order to explain the different band structures of AZ and AA' structures we calculated the charge density associated to the bands of the doped (5,5) SWNTs. It is obtained by summation over all k-points of the square of the absolute value of the wavefunctions for a given band. We analyze N doped structures but the conclusions are analogous for B doping. As it can be verified from figure 5 in AZ isomer the charge density associated to the conduction band is more delocalized than in AA' isomer because the distance of N impurities along the longitudinal direction in the first structure is the half of the second one (4.88 Å and 9.76 Å, respectively). Therefore the delocalization of the density of charge associated to the conduction band is reflected in the band crossing of AZ isomer, which makes the SWNT metallic. In other words we found that in doped (5,5) SWNT the electronic properties depend not only on the concentration of impurities, but even on how they are distributed along SWNT.

We point out that N and B doped (5,5) SWNTs have equivalent electronic behaviors in the electron and hole descriptions, respectively. As a matter of fact, valence (conduction) band of the N doped SWNT has the same width and behaviour of the conduction (valence) band of the B doped SWNT and also the same gap, if it is present. This finding is a direct consequence of the symmetry of the bands of the pure (5,5) SWNT with respect to the Fermi energy. Instead the bands of the pure (8,0) SWNT are not symmetrical with respect to Fermi energy and N and B doped SWNTs show band structures with distinct features and different occupation. We conclude that holes and electrons have asymmetrical behaviors in (8,0) zig-zag SWNT.

4. Conclusions

N and B doping of (8,0) and (5,5) SWNTs have been investigated by first principles calculations for two different isomers (AZ and AA'), where we have inserted two impurities of the same type per unit cell. The electronic band structures we have calculated exhibit a strong hybridization with impurity orbitals that upsets the original band structures.

The formation energies of the two isomers are very similar for any type of doping. Nevertheless band structures of the (5,5) SWNT isomers are different. Indeed, AZ isomer is gapless and exhibit a crossing of fully occupied valence band and empty conduction band, while band structures of AA' isomer exhibit an energy gap (0.4 eV within GGA) above valence band. Our calculations showed that density of charge associated to the conduction band is more delocalized for AZ isomer, where the distance of the N impurities along longitudinal direction is 4.88 Å, that is the half of same distance in AA' isomer. Similar results hold for B doping. We conclude that the band crossing of AZ isomer is due to the delocalization of the density of charge that leads to metallic behaviors, as deduced from the analysis of the DOS.

The bands of the pure (8,0) SWNT are not symmetrical with respect to the Fermi energy differently from (5,5) SWNT so for an assigned isomer N and B doping present band structures with distinct features and different occupation. We found that in the N doped (8,0) SWNT the bands are just partially occupied, while in the B doped case the Fermi energy is shifted downward to the top of the new valence band and the doped SWNT exhibit a negligible indirect energy gap. From the analysis of the DOS we deduced that both B doped isomers are metals. This finding let us conclude that holes and electrons have asymmetric behaviors in zig-zag (8,0) SWNT. The present work shed light on aspects of the electronic structures of doped SWNTs not evidenced in previous works. An extension of the analysis we have performed to other SWNTs with different radius and chirality could be useful in order to generalize our results.

Acknowledgments

I thank my colleague Dr. Vincenzo Vinciguerra, and Dr. Giovanni Cantele and Dr. Fabio Trani of the Università di Napoli Federico II for useful discussions. I thank G. C. for careful reading of the manuscript.

Bibliography

[1] J. C. Charlier, M. Terrones, M. Baxendale, V. Meunier, T. Zacharia, N. L. Rupesinghe, W. K. Hsu, N. Grobert, H. Terrones and G. A. Amaratunga, *J Nano Lett.* **2** 1191 (2002)

[2] D. Golberg, Appl. Phys. A **73** 499 (2003)

[3] Y. Zhang, D. Zhang and C. Liu, J. Phys. Chem. B **110**, 4671 (2006)

[4] P. E. Lammert, V. H. Crespi and A. Rubio, Phys. Rev. Lett. **87** 136402 (2001)

[5] A. H. Nevidomskyy, G. Csányi and M. C. Payne, Phys. Rev. Lett. **91** 105502 (2003)

[6] O. Stephan, P. M. Ajayan, C. Colliex, P. Redlich, J. M. Lambert, P. Bernier and P. Lefin, Science **266** 1683 (1994)

[7] P. Redlich, J. Loeffler, P. M. Ajayan, J. Bill, F. Aldinger and M. Rühle, Chem. Phys. Lett. **260** 465 (1996)

[8] M. Terrones, W. K. Hsu, S. Ramos, R. Castillo and H. Terrones, Fullerene Sci. Technol. **6** 787 (1998)

[9] M. Glerup, J. Steinmetz, D. Samaille, O. Stephan, S. Enouz, A. Loiseau, S. Roth and P. Bernier, Chem. Phys. Lett. **387** 193 (2004)

[10] P. L. Gai *et al,* J. Mater. Chem. **14** 669 (2004)

[11] M. Terrones *et al,* Chem. Phys. Lett. **259** 568 (1996)

[12] M. Terrones *et al,* Nature **388** 52 (1997)

[13] M. Terrones *et al,* Adv. Mater. **11** 655 (1999)

[14] R. Sen, B. C. Sathishkumar, S. Govindaraj, K. R. Ravikumar, M. K. Renganathan and C. N. R. Rao, J. Mater. Chem. **7** 2335 (1997)

[15] L. H. Chan, K. H. Hong, D. Q. Xiao, T. C. Lin, S. H. Lai, W. J. Hsieh and H. C. Shih, Phys. Rev. B **70** 125408 (2004)

[16] R. Crzew *et al,* Nanoletters **1** 457 (2001)

[17] J. Kotakoski, A. V. Krasheninnikov, Y. Ma, A. S. Foster, K. Nordlund and R. M. Nieminen, Phys. Rev. B **71** 205408 (2005)

[18] K Yamamoto, T. Kamimura and K. Matsumoto, Jpn. J. Appl. Phys. **44** 1611 (2005)

[19] H. S. Kang and S. Jeong, Phys. Rev. B **70** 233411 (2004)

[20] M. Perdew, K. Burke and M. Ernzerhof, Phys. Rev. Lett. **77** 3865 (1996)

[21] B. Delley, J. Chem. Phys. **92**, 508 (1990); B. Delley, J. Chem. Phys. **113** 7756 (2000). DMol^3 program is available from Accelrys Inc.: http://www.accelrys.com.

[22] J. Andzelm, D. King-Smith and G. Fitzgerald, Chem. Phys. Lett. **335**, 321 (2001)

[23] H. J. Monkhorst and J. D. Pack, Phys. Rev. B **13**, 5188 (1976)

[24] G. J. Ackland, Phys. Rev. Lett. **80** 2233 (1998)

[25] R. Saito, M. S. Dresselhaus and G. Dresselhaus, Physical Properties of Carbon Nanotubes (Imperial College Press, London, 1998).

Tables

	AA' isomer (eV)	AZ isomer (eV)
N doped	7.00	6.96
B doped	4.11	3.98

Table 1: Formation energy of doped (8,0) SWNT

	Pure X=C	AA' isomer X=N	AZ isomer X=N	AA' isomer X=B	AZ isomer X=B
X-C_1	1.404	1.375	1.376	1.494	1.493
X-C_2	1.430	1.430	1.432	1.515	1.519

Table 2: Lengths of X-C bonds (in Ångstrom) in (8,0) SWNT. C atoms labeled 1 and 2 are indicated in figure 1.

	AA' isomer (eV)	AZ isomer (eV)
N doped	6.95	6.94
B doped	3.35	3.37

Table 3: Formation energy of doped (5,5) SWNT

	Pure X=C	AA' isomer X=N	AZ isomer X=N	AA' isomer X=B	AZ isomer X=B
X-C_1	1.436	1.407	1.411	1.520	1.520
X-C_2	1.415	1.411	1.410	1.496	1.496

Table 4: Lengths of X-C bonds (in Ångstrom) in (5,5) SWNT. C atoms labeled 1 and 2 are indicated in figure 1.

Captions

Figure 1. The unit cells of the N or B doped SWNTs. In a) and b) AZ and AA' isomers are shown for (5,5) SWNT, respectively. In c) and d) AZ and AA' isomers are shown for (8,0) SWNT, respectively.

Figure 2. One-dimensional band structures of (a) substitutive N doped, (b) pure and (c) substitutive B doped (8,0) SWNT. In (a) and (c) full lines correspond to the AZ isomer and

dashed lines to the AA' isomer (see figure 1). The impurity band labels F and G are referred to both isomers. The Fermi energy is located at E_F= 0 eV.

Figure 3. Density of states of (a) AZ isomer (full line) and AA' isomer (dashed line) of B doped (8,0) SWNT and (b) AZ isomer of N doped (full line) and B doped (dashed line) (5,5) SWNT.

Figure 4. One-dimensional band structures of (a) substitutive N doped, (b) pure and (c) substitutive B doped (5,5) SWNT. Bands reported as full lines correspond to AZ isomer, while dashed bands corresponds to AA' isomer with reference to figure 1. The AA' isomer band structure of both B and N doped SWNT exhibit an energy gap, not present in AZ isomer.

Figure 5. Isosurfaces of the charge density associated to the conduction band of a) AZ and b) AA' isomers of doped (5,5) SWNT. The plotted isosurfaces correspond to the 20% of the maximum of the charge density.

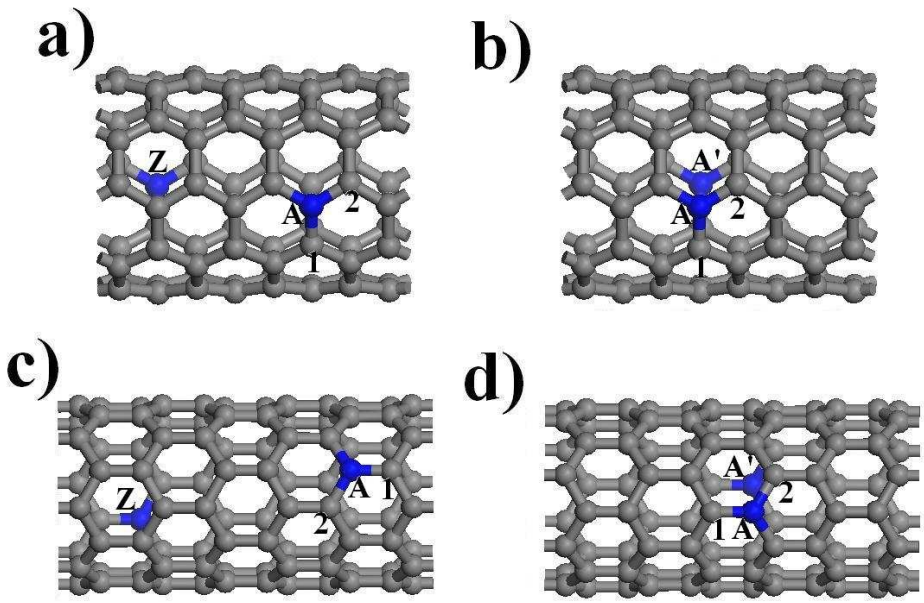

306x212mm (96 x 96 DPI)

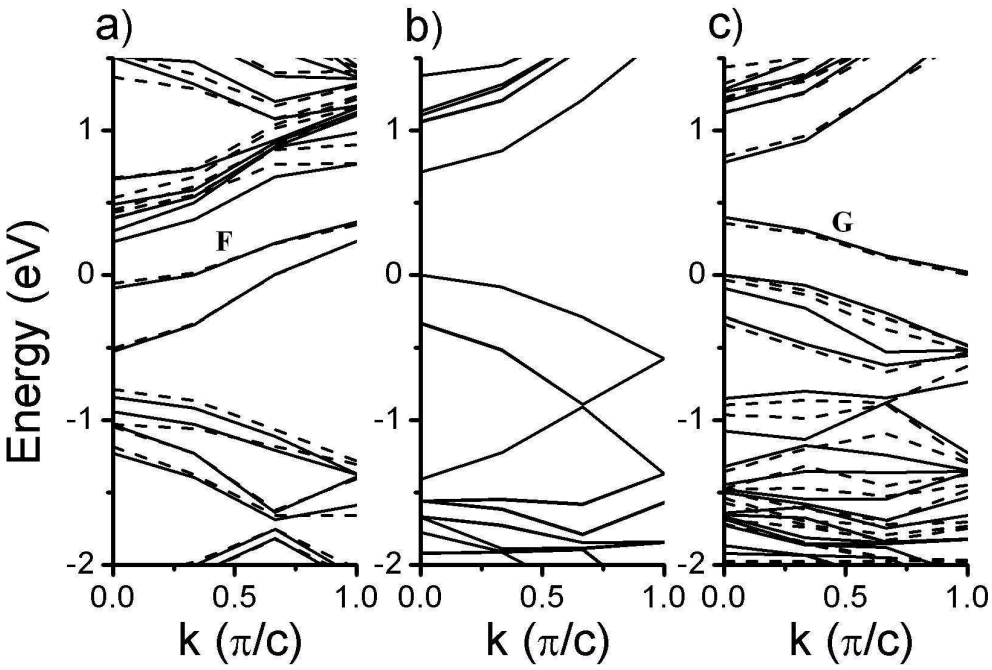

438x307mm (96 x 96 DPI)

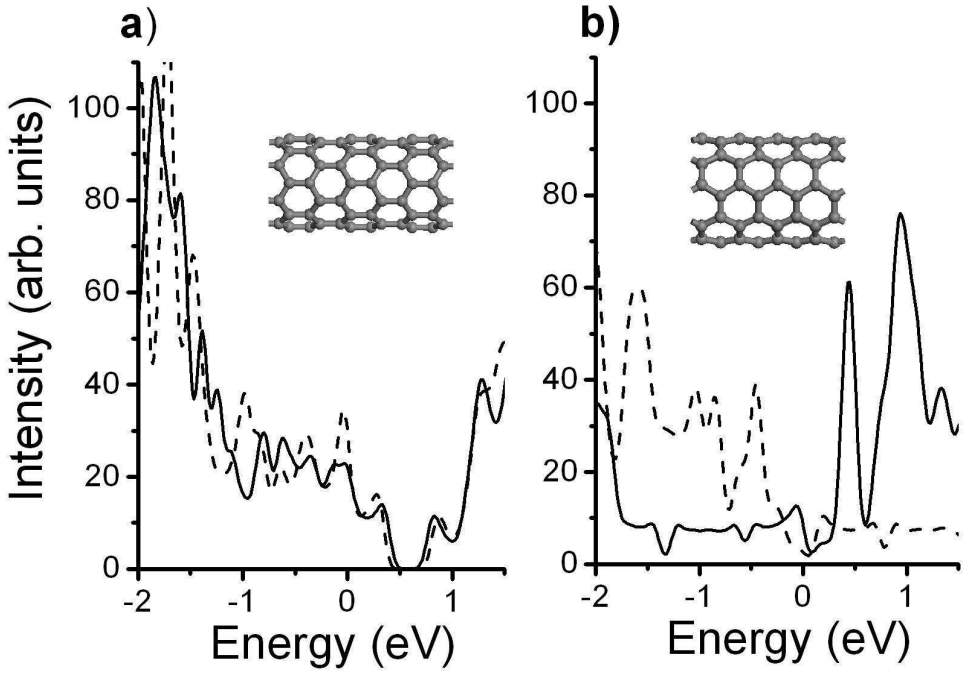

438x307mm (96 x 96 DPI)

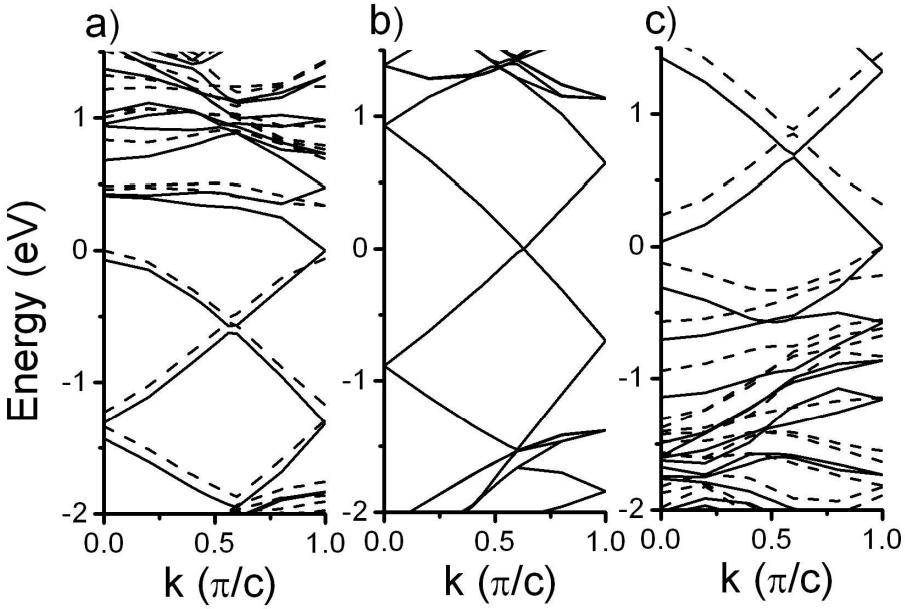

308x216mm (150 x 150 DPI)

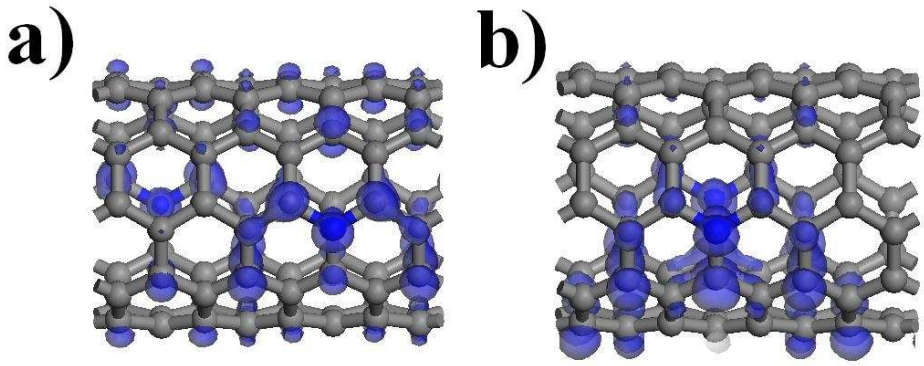

290x169mm (96 x 96 DPI)